

SPANWISE LARGE SCALE MOTIONS AND THEIR RELATION TO ENERGY SPECTRUM IN TURBULENT SHEAR FLOWS

Yu Wang

Department of Energy Engineering and Science
Nagoya University
Furo-Cho, Chikusaku, Nagoya city, 464-8603, Japan
wang.yu.k7@s.mail.nagoya-u.ac.jp

Yoshinobu Yamamoto

Department of Mechanical Engineering
University of Yamanashi
4-3-11, Takeda, Kofu 400-8511, Japan
yamamotoy@yamanashi.ac.jp

Yoshiyuki Tsuji

Department of Energy Engineering and Science
Nagoya University
Furo-Cho, Chikusaku, Nagoya city, 464-8603, Japan
c42406a@nucc.cc.nagoya-u.ac.jp

ABSTRACT

Studies on the structure of turbulent boundary layer have attracted a significant amount of attention in the last few decades, it has been recognized that wall turbulence is composed of certain recurring and quantifiable features collectively referred to as ‘coherent structures’. Kline *et al.* (1967) observed the presence of streak structures in the viscous sub-layer by flow field visualization. And recently, with the development of fluid measurement technology and fluid simulation technology, there are many studies on the large-scale structure in boundary layer (Kim & Adrian (1999); Ganapathisubramani *et al.* (2003)). And there has been an increasing interest in the statistical analysis of small-scale close to the wall and study of large-scale features, especially in boundary layers, Hutchins & Marusic (2007*b*) reported the presence of very long meandering structures in turbulent boundary layers, which they called ‘super-structures’, whose length can reach to 20δ . Although a great deal of research has been conducted on large scale structures, there are still many unknown points, However, there are relatively few studies on the characteristics of span-wise direction of the turbulent structure. In this paper, the flow field is decomposed using specific thresholds (along the span-wise direction, the thresholds used are described later), and the large scale components defined in this paper are analytically discussed to have a significant contribution to the formation of the outer peaks of the velocity pre-multiplied spectrum by calculating the flow field pre-multiplied spectrum.

THE NUMERICAL AND EXPERIMENTAL DATA

The experiment was conducted in a channel wind tunnel and the results of the numerical simulations were obtained from Yamamoto & Tsuji (2018), Most of the detailed discussions are based on the turbulence channel simulations of Yamamoto & Tsuji (2018).

And the experimental facility consist of wind tunnel and hot-wire anemometer. The channel wind tunnel is blowout type wind tunnel, which consisting of a blower, a rectifier, and a test section. A dust collection filter is attached to the suction part of the blower, which removes the dust from the air.

The velocity fluctuation is measured by the hot-wire operated by constant temperature anemometer. It is attached to the traverse devise and the velocity distribution is obtained across the test section. In the channel flow, the distance from the wall was measured by 84 points from $0mm$ to $25mm$. The hot-wire rake made of 16 single I-probe was used in the measurement. I-type probe is made of tungsten wire with the sensor length, and its diameter is $\phi = 5\mu m$. The probes are arranged in the span-wise direction, and the spacing between each probe is $4mm$. The total span-wise extent of the probes is $l = 60mm$, and it is approximately 2.4δ (δ is the channel half wall-height). The hot-wire origin was placed slightly away from the wall not to damage the wire due to the interaction with the wall. The sampling frequency is 20 kHz , and the data are recorded for 60 seconds at each measurement position. In this paper, we compare the results of experimental and numerical simulations. The experimental data were obtained from measurements with a hot-wire anemometer, the details of which are summarized in Table 1.

In this paper, the coordinates x , y , and z present the stream-wise, span-wise, and wall-normal direction, respectively. In channel, we defined that the boundary layer thickness is regarded as channel’s half height (that is, $\delta = h$). The upper superscript $+$ indicates a non-dimensional values such as wavelength $\lambda^+ = \lambda_x u_\tau / \nu$ and velocities $u^+ = u / u_\tau$, where ν is the kinematic viscosity.

MEAN VELOCITY AND TURBULENT INTENSITY PROFILE

Mean velocity and turbulent intensity profiles are plotted in Fig. 1 and Fig .2. In this study, the hot-wire array consisting of 16 I-probes arranged in the span-wise direction was used. The distance between adjacent probes is $4mm$. The velocity profiles and turbulence intensity profiles of the random one probe and numerical simulations are shown in Fig. 1 and Fig .2. The distance between probes is $4mm$ and the spatial resolution is not sufficient, which results in a discrepancy between the experimental and numerical simulation values in the turbulence intensity profile. In comparison with DNS, the mea-

Table 1: Parameter of data setup. L_x and L_z are the periodic stream-wise and span-wise dimensions of the numerical box, and h is the channel half height. N_x , N_y , and N_z are the grid points, where x indicates the stream-wise, y indicates the wall-normal, and z indicates the span-wise direction.

Name	line	Source	Re_τ	L_x/h	L_z/h	Δx^+	Δz^+	N_x	N_y	N_z
case1	—	Experimental	930	—	—	—	—	—	—	—
case2	--	Simulation	1000	12.8	6.4	13.33	8.33	960	512	768
case3	---	Simulation	2000	12.8	6.4	16	8.33	2000	1024	1536

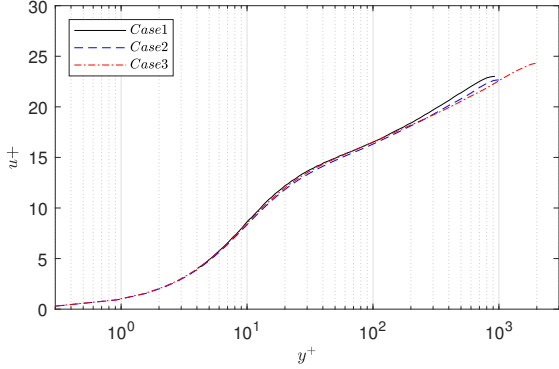


Figure 1: Mean velocity profiles. case1 — experimental $Re_\tau = 930$; case2 -- simulation $Re_\tau = 1000$; case3 - - - simulation $Re_\tau = 2000$.

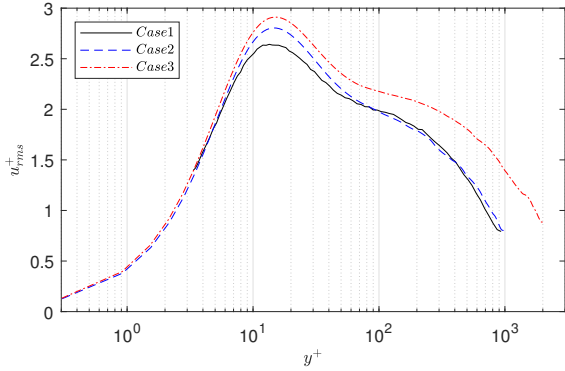


Figure 2: Turbulent intensity profiles. case1 — experimental $Re_\tau = 930$; case2 -- simulation $Re_\tau = 1000$; case3 - - - simulation $Re_\tau = 2000$.

surement underestimates the turbulent intensity (or RMS, root mean square) near the wall region. This is not due to the probe interaction among 16 ch probes, but attributes to the space resolution of sensor length of hot-wire. Since this paper focus on the turbulent large-scale structure, the discrepancy can be neglected and does not influence the results of this study.

SPAN-WISE WIDTH SCALE

From previous studies, we know that in the contour figures of velocity fluctuations at different wall heights, there exist low and high velocity regions (Monty *et al.* (2007)), which

are usually represented as meandering elongated structures on the contour maps. The low velocity region is flanked by the high velocity region, which is characteristic of the very large scale motion (VLSM) from Hutchins & Marusic (2007b). But only qualitative conclusions can be drawn from these figures. Therefore a statistical analysis is required to determine the average structural characteristics. Eq. 1 gives the definition of the two-point correlation along the span direction for quantifying the span-wise scales of turbulent large-scale structures.

$$R_{uu}(\Delta z') = \frac{\langle u'(z, t)u'(z + \Delta z', t) \rangle}{\langle u'(z, t)^2 \rangle} \quad (1)$$

Here, u' is the velocity fluctuating component and the angle brackets indicate time average, while z is the coordinate along the probe or span-wise direction, $\Delta z'$ indicates the distance along span-wise direction, and R_{uu} indicates the two-point correlation along the span direction.

Figure 3 shows the result of two-point correlation of stream-wise velocities at eight different wall heights. The data are from case2, $Re_\tau = 1000$. And Fig. 4 shows the result of case3, simulation data, $Re_\tau = 2000$. The span-wise typical scale l_s is defined by the two-point correlation function. It is the distance between the points where R_{uu} has a small positive value (but not zero). According to Monty *et al.* (2007), we adopt a threshold of $R_{uu} = 0.05$, and this correlation threshold is marked on Fig. 3 and Fig. 4 with a dashed line. The value of l_s is indicated by the double arrow in the figure. We can see that in the channel flow (both experimental and simulations result) the value of l_s becomes larger with the increase of the wall height, and it is worth noting that the increase of the width of the turbulent structure is also manifested in the boundary layer flow (Hutchins *et al.* (2005); Adrian *et al.* (2000)). Fig. 5 represents the variation of l_s relative to the wall height at different Reynolds numbers, and the variation of l_s at three cases is given on the way, corresponding to the results of experimental and numerical simulations at different Reynolds numbers. The horizontal coordinate in Fig. 5 indicates the wall distance and the vertical coordinate indicates the value of l_s , which is normalized by the boundary layer thickness δ . We can observe that the variation of l_s at different Reynolds numbers is consistent. And it shows different growth rates near the wall and away from the wall, and the wall height is about $y/\delta \sim 0.12$ when the growth rate changes.

It is assumed that l_s grows linearly, although it presents different growth rates near and away from the wall (in agreement with Monty *et al.* (2007) results, although the wall height where the growth rate changes does not agree with each other). Outside of logarithmic region, the width of turbulent

Table 2: Definition of filter parameters for velocity decomposition in span-wise direction. Notation u' denotes the original component; u'_L denotes the large scale; and u'_s denotes the small scale component of velocity fluctuation.

Notation	Designation	Cutoff
u'	original component	—
u'_L	large-scale component	$\lambda_z/l_s^* > 1$
u'_s	small-scale component	$\lambda_z/l_s^* < 1$

span-wise structures grows at a different rate up to the center of the channel. In this paper, the velocity field is decomposed into large and small scale components by the filtering of span-wise wave length $2l_s$. This length scale is two times of l_s where the growth rate changes.

VELOCITY DECOMPOSITION

In this paper the threshold is represented by $l_s^* = 2 \times l_s$ (it is equal to the value of $2l_s$ at $y/\delta = 0.12$). The stream-wise velocity fluctuations whose span-wise wave length is larger than l_s^* are denoted as large scale components u'_L . The stream-wise velocity fluctuations whose span-wise length scale is smaller than l_s^* are denoted as small scale components u'_s . Scaled decomposition are summarized in Table 2. They are expressed by Eq .2.

$$u' = u'_L + u'_s \quad (2)$$

Figure 6, 7 and 8 are examples of the decomposition of velocity fluctuations in the channel of experimental data and DNS data, respectively. Each figure represents an contour surface map of velocity fluctuations for different velocity components, (a) original velocity component, (b) large-scale velocity component, and (c) small-scale velocity component. In this contour plot, the blue color indicates the low velocity region and the red color indicates the high velocity region. We can see that the blue low velocity zone and the red high velocity zone in the different velocity components meander alternately with each other along the flow direction. In the following, we analyze the one-dimensional velocity pre-multiplied spectra for the stream-wise direction of u' , u'_L and u'_s .

PRE-MULTIPLIED SPECTRUM

By comparing the large-scale and the small-scale component, we defined the presence of a large-scale structure fluctuating in the span-wise direction in the large-scale component and the absence of such a structure in the small-scale component. In this section, we will consider the pre-multiplied energy spectra (PMS) of stream-wise velocity fluctuation of different velocity components of case1, case2 and case3. The spectral density function of the stream-wise velocity fluctuation ϕ_{uu} is used and the stream-wise wavelength and wave-number are denoted by λ_x and k_x ($k_x = 2\pi/\lambda_x$), and $k_x\phi_{uu}$ represent the pre-multiplied energy spectra of stream-wise velocity fluctuation. In this study all of the data are presented in

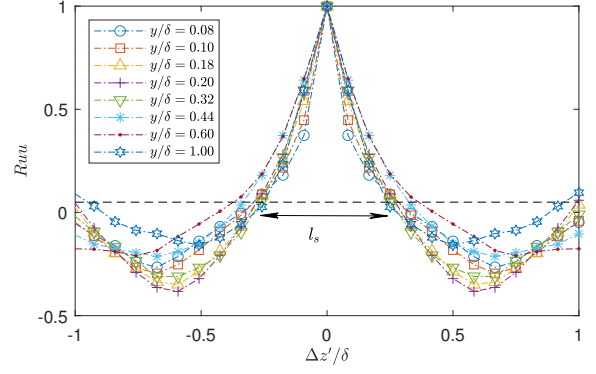


Figure 3: Two-point correlations for eight different wall heights. Data from case2, simulation $Re_\tau = 1000$; Different symbols indicate different wall heights.

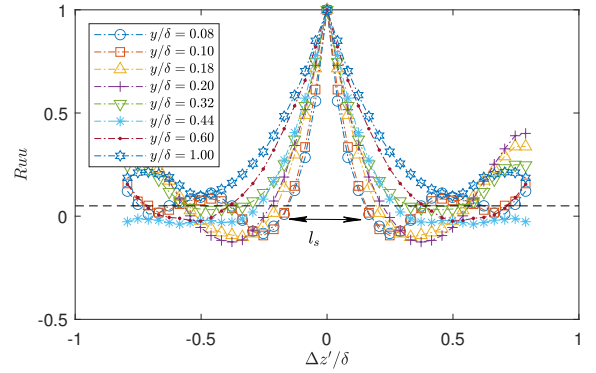


Figure 4: Two-point correlations for eight different wall heights. Data from case3, simulation $Re_\tau = 2000$; Different symbols indicate different wall heights.

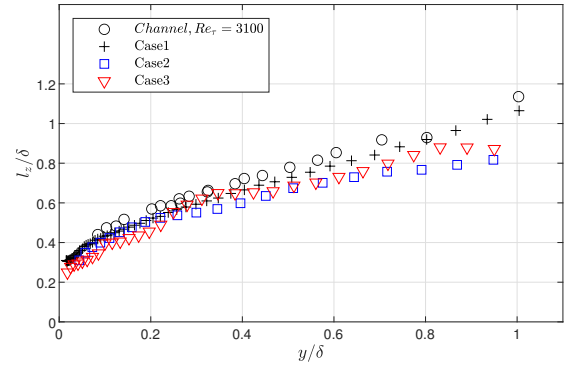


Figure 5: Variation of span-wise width scale, l_s , with wall distance. \circ , data of channel from Monty *et al.* (2007), $Re_\tau = 3100$; $+$ denotes case1; \square denotes case2; ∇ denotes case3.

terms of stream-wise length-scale λ_x^+ . Figure 9 shows the Pre-multiplied energy spectrum results of case1, case2 and case3. In Fig. 9, the different cases are represented horizontally as case1, case2 and case3. and the different velocity components u' , u'_L and u'_s are represented vertically.

In previous study (Hutchins & Marusic (2007a,b)). The 'inner site' and 'outer site' are defined, where 'inner site' is

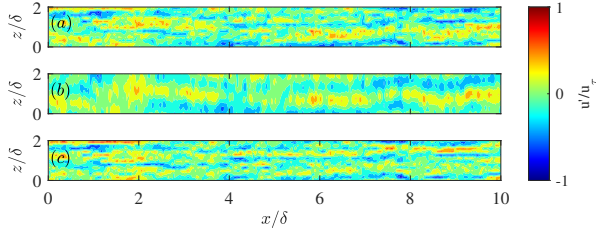


Figure 6: Example of the contour map of velocity fluctuations in channel of case1, $Re_\tau = 930$, normalized by friction velocity u_τ , and the wall-height is $y/\delta = 0.08$. (a)original velocity component; (b)large-scale velocity component u'_L ; (c)small-scale velocity component u'_s .

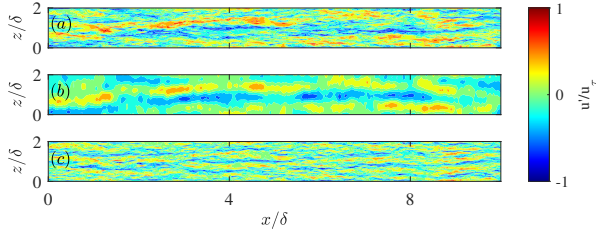


Figure 7: Example of the contour map of velocity fluctuations in channel of **case2**, $Re_\tau = 1000$, normalized by friction velocity u_τ , and the wall-height is $y/\delta = 0.08$. (Same as Fig. 6).

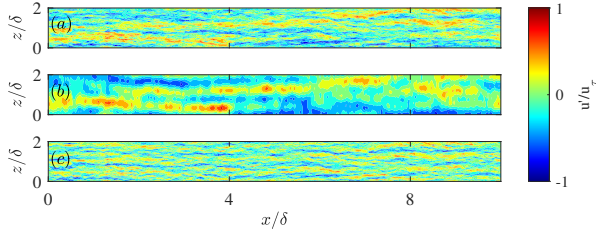


Figure 8: Example of the contour map of velocity fluctuations in channel of **case3**, $Re_\tau = 2000$, normalized by friction velocity u_τ , and the wall-height is $y/\delta = 0.08$. (Same as Fig. 6).

a near-wall energy peak, and that this peak is approximately fixed in viscous coordinates at $y^+ = 15$ and $\lambda^+ = 1000$, and 'outer site' has a clear peak in the pre-multiplied spectra at length-scales that are many times larger than the boundary-layer thickness ($\lambda_x \approx 6\delta$). And the wall height is $z^+ = 3.9\sqrt{Re_\tau}$ (consistent with the nominal area of log region, and expressed in the coordinates of this study as $y^+ = 3.9\sqrt{Re_\tau}$) (Mathis *et al.* (2009)). The position of the inner site (or inner peak) and its corresponding wavelength are fixed, while the outer site (or outer peak) is related to the Reynolds number. It is at high Reynolds number ($Re_\tau \geq 1700$) that the near-wall and logarithmic region can be clearly distinguished, seeing at least a decade separation (one order of magnitude) between the two energy points.

In cases 1 and 2, where the Reynolds number is around 1000, it is difficult to see a clear separation between the inner and outer peaks, and even in case 3, the outer peaks are

difficult to observe. Based on the decomposition method in this study, in the large-scale velocity component, (u'_L in Fig .9), for the experimental case the outer peak becomes obvious, but the inner layer peak still exists. For the numerical simulation results, the large-scale velocity component has no inner layer peak and only shows the characteristics of the outer layer peak. Regarding the small-scale components, (u'_s in Fig .9), for different cases (case1, case2 and case3), the velocity pre-multiplied spectra corresponding to the small-scale components all have only the inner peaks. Taking into account the definition of the large-scale and the small-scale velocity decomposition, we can draw an interesting conclusion: The large-scale velocity components defined in this paper have an important role in the generation of the outer peaks of the PMS, and the velocity decomposition threshold, l_s^* , defined in this paper, can be considered as the characteristic length for the separation of the inner and outer peaks of the stream-wise velocity.

In previous studies, meandering structures exist in the turbulent boundary layer up to 20δ in length, called Very large scale motion (VLSM) (Balakumar & Adrian (2007); Kim & Adrian (1999)), and are associated with the generation of the outer peaks of PMS, which are similar to the u'_L defined in this paper, and it can be considered that the threshold (l_s^*) defined in this paper separates out the VLSM turbulent structures.

CONCLUSION

In this paper, the width scale l_s in the span-wise direction is defined by the data from experiments and numerical simulations in the channel flow, through the calculation of cross correlation coefficients, based on previous studies by Monty *et al.* (2007). l_s increases with the distance from the wall and grows linearly, but shows different growth rates near the wall and away from the wall. In this paper, two times of l_s chosen as the threshold to decompose the flow field. Through a simple Fourier filter and extraction of velocity components, velocity components with different wavelengths in the span-wise direction are obtained. By comparing the relationship of large-scale components and the small-scale components. The PMS of different scale is compared through statistical methods, and the following conclusions are obtained:

- The outer peaks of the PMS contour appear even at low Reynolds number, and they are due to the structure of the long wavelength velocity component that fluctuates or meanders in the span-wise direction.
- The threshold l_s^* for the velocity field decomposition defined in this paper can be considered to decompose the velocity components containing span wavelengths larger than l_s^* and span wavelengths smaller than l_s^* , where u'_L , which can be considered as the VLSM defined in previous studies (as a conjecture), has a distinct outer peak in its velocity pre-multiplied spectrum.
- It was clarified that the fluctuation of the large-scale structure in the span-wise direction and the effective usefulness of the energy are deeply related.
- Regarding the distance from the wall when the growth rate of l_s varies, the results of this paper differ from those of previous studies Monty *et al.* (2007), the results of this paper are closer to the wall with $y/\delta = 0.1$. However this location indicates the position where the growth rate changes.

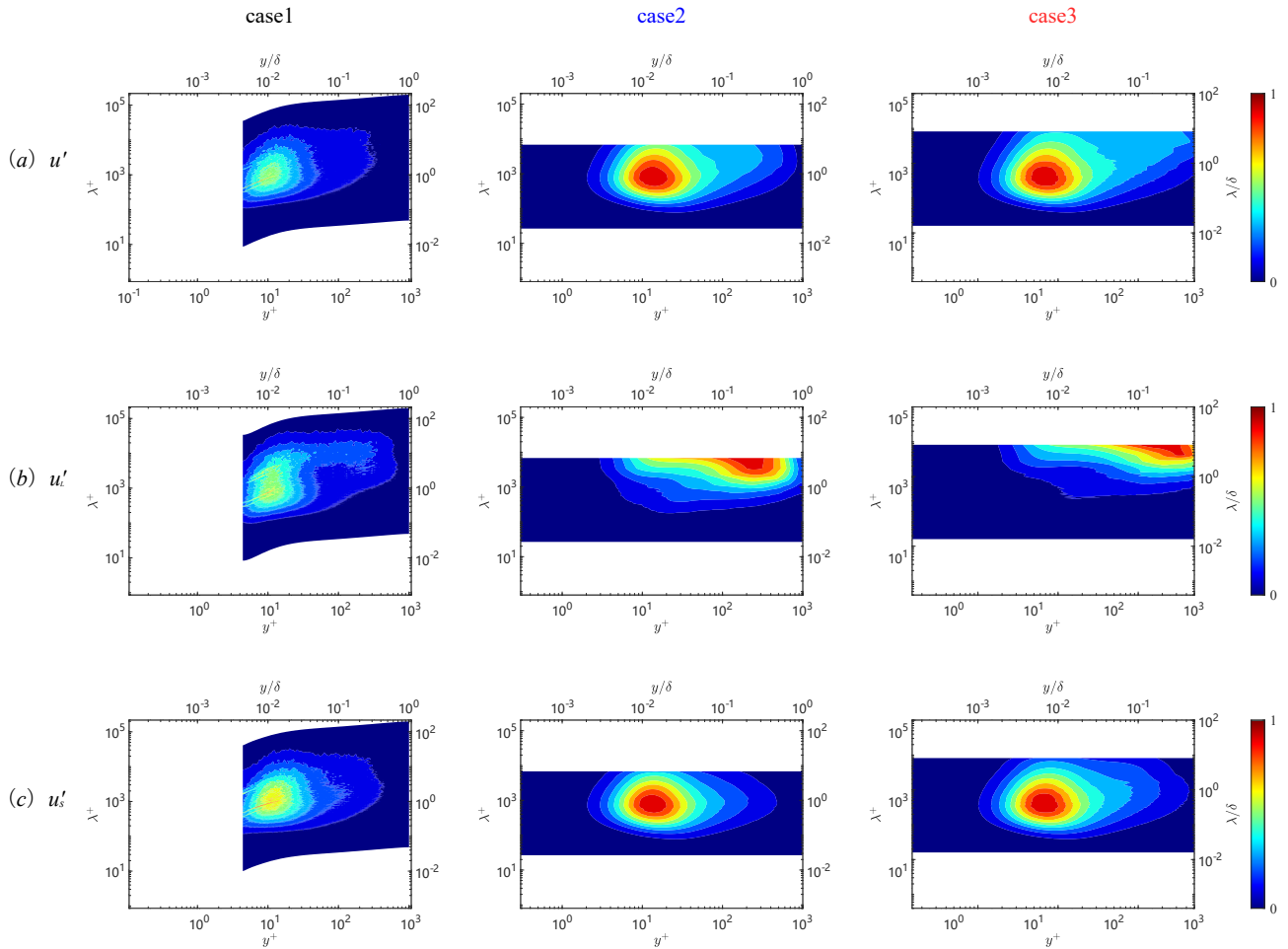


Figure 9: Pre-multiplied one-dimensional spectra $k_x \phi_{uu} / \max(\phi_{uu})$ as function of wavelength and wall distance, case1, experimental; case2, simulation $Re_\tau = 1000$; case3, simulation $Re_\tau = 2000$. The vertical figure represents the different velocity components u' , u'_L and u'_s .

ACKNOWLEDGMENTS

This work was financially supported by JST SPRING, Grant Number JPMJSP2125. The author (Initial) would like to take this opportunity to thank the “Interdisciplinary Frontier Next-Generation Researcher Program of the Tokai Higher Education and Research System.”

This work is partially supported by “Nagoya University High Performance Computing Research Project for Joint Computational Science” in Japan. This work was supported by JSPS KAKENHI Grant Number 19H00747.

REFERENCES

- Adrian, Ronald J, Meinhart, Carl D & Tomkins, Christopher D 2000 Vortex organization in the outer region of the turbulent boundary layer. *Journal of fluid Mechanics* **422**, 1–54.
- Balakumar, BJ & Adrian, RJ 2007 Large-and very-large-scale motions in channel and boundary-layer flows. *Philosophical Transactions of the Royal Society A: Mathematical, Physical and Engineering Sciences* **365** (1852), 665–681.
- Ganapathisubramani, Bharathram, Longmire, Ellen K & Marusic, Ivan 2003 Characteristics of vortex packets in turbulent boundary layers. *Journal of Fluid Mechanics* **478**, 35–46.
- Hutchins, N, Hambleton, WT & Marusic, Ivan 2005 Inclined cross-stream stereo particle image velocimetry measurements in turbulent boundary layers. *Journal of Fluid Mechanics* **541**, 21–54.
- Hutchins, N & Marusic, Ivan 2007a Evidence of very long meandering features in the logarithmic region of turbulent boundary layers. *Journal of Fluid Mechanics* **579**, 1–28.
- Hutchins, Nicholas & Marusic, Ivan 2007b Large-scale influences in near-wall turbulence. *Philosophical Transactions of the Royal Society A: Mathematical, Physical and Engineering Sciences* **365** (1852), 647–664.
- Kim, Kyung Chun & Adrian, Ronald J 1999 Very large-scale motion in the outer layer. *Physics of Fluids* **11** (2), 417–422.
- Kline, Stephen J, Reynolds, William C, Schraub, FA & Runstadler, PW 1967 The structure of turbulent boundary layers. *Journal of Fluid Mechanics* **30** (4), 741–773.
- Mathis, Romain, Hutchins, Nicholas & Marusic, Ivan 2009 Large-scale amplitude modulation of the small-scale structures in turbulent boundary layers. *Journal of Fluid Mechanics* **628**, 311–337.
- Monty, JP, Stewart, JA, Williams, RC & Chong, MS 2007 Large-scale features in turbulent pipe and channel flows. *Journal of Fluid Mechanics* **589**, 147.
- Yamamoto, Yoshinobu & Tsuji, Yoshiyuki 2018 Numerical evidence of logarithmic regions in channel flow at $Re_\tau = 8000$. *Physical Review Fluids* **3** (1), 012602.